AIMS Mathematics, 9(7): 18589–18607.
DOI:10.3934/math.2024905
Received: 28 January 2024
Revised: 17 April 2024
Accepted: 23 April 2024
Published: 03 June 2024

https://www.aimspress.com/journal/Math

Research article

Generalized logistic model with time-varying parameters to analyze COVID-19 outbreak data

Said Gounane[1], Jamal Bakkas[2], Mohamed Hanine[3], Gyu Sang Choi[4,*] and Imran Ashraf[4,*]

[1] Laboratory of MIMSC, Cadi Ayyad University, Higher School of Technology, Essaouira, Morocco

[2] LAPSSII Laboratory, Graduate School of Technology, Cadi Ayyad University, Safi, Morocco

[3] Department of Telecommunications, Networks, and Informatics, LTI Laboratory, ENSA, Chouaib Doukkali University, Eljadida, Morocco

[4] Department of Information and Communication Engineering, Yeungnam University, Gyeongsan 38541, Republic of Korea

* **Correspondence:** Email: castchoi@ynu.ac.kr, imranashraf@ynu.ac.kr.

Abstract: Accurately estimating the number of infections that actually occur in the earliest phases of an outbreak and predicting the number of new cases per day in various countries is crucial for real-time monitoring of COVID-19 transmission. Numerous studies have used mathematical models to predict the progression of infection rates in several countries following the appearance of epidemiological outbreaks. In this study, we analyze the data reported and then study several logistical-type phenomenological models and their application in practice for forecasting infection evolution. When several epidemic waves follow one another, it is important to stress that a traditional logistic model cannot necessarily be fully adapted to the data made available. New models are being introduced to simultaneously take account of human behavior, measures taken by the government, and epidemiological conditions. This research used a generalized logistic model based on parameters that vary over time to describe trends in COVID-19-infected cases in countries that have undergone several waves. In two-wave scenarios, the parameters of the model evolve dynamically over time following a logistic function, where the first and second waves are characterized by two extreme values for the early period and the late one, respectively.

Keywords: logistic model; generalized Richards model; time-dependent parameters; multiple cycle models; infected cases; COVID-19 outbreak

1. Introduction

The emergence of COVID-19, the latest global pandemic following SARS in 2003 and MERS in 2012, poses a significant threat to both human health and the global economy. COVID-19 belongs to the coronavirus family and causes SARS in those infected. The virus is primarily transmitted through coughing or sneezing on others. Governments worldwide have implemented drastic restrictions to curb the spread of the virus, including strict health and economic policies tailored to this global health emergency. However, slow-developing countries and emerging economies may not be able to implement similar measures as developed countries. The pandemic had a significant impact on employment, resulting in reduced production, trade barriers, global demand, and restrictions on movement. Due to the lack of a clear understanding of the pandemic's evolution in almost every country, health officials have had to carry out strict policies to control the outbreak. Therefore, this global health crisis highlights the crucial significance of scientific research, especially the use of practical approaches, which are both efficient and lightweight to comprehensively model and assimilate reported data to understand the disease's spread over time.

Modeling long-term predictions based on reported data from other countries is necessary but challenging. To describe the temporal and spatial evolution of the COVID-19 pandemic, several mathematical models covering deterministic models, stochastic models, and both discrete-time and continuous-time models have been developed, with varying degrees of complexity [1]. Health authorities are increasingly relying on mathematical, statistical, and artificial intelligence techniques to control infectious disease epidemics [2]. Mathematical models are now commonly used to forecast the spread and dynamics of infection, determine the principle transmission pathways to be used in the control, evaluate the effectiveness of precautionary measures to be expected like lockdown and social distancing, as well as predict the impact of measures taken and the progression of epidemics [3–6]. Using mathematical models can help strategic decision-making to allocate optimal resources and treatment facilities to ensure effective control of infectious disease outbreaks. Taking a look at short-term forecasts can help to estimate and anticipate requirements in terms of material and human resources. Nevertheless, disease transmission forecasts may be quickly overtaken because of the fast evolution of transmission rates strongly impacted by population attitude changes, environmental factors, and the effectiveness of control measures taken.

It is challenging to study the multiple waves that occur during an epidemic and requires appropriate models to characterize the complex growth patterns that occur in epidemic curves. COVID-19 data may present non-linear trends due to the nature of the dynamic evolution of the pandemic as well as the measures applied, which may not be well captured by classical logistic models. On the other hand, different waves of the pandemic may present distinct temporal characteristics, such as variable growth rates, different time periods, and changing government interventions, which can make it difficult to apply simple logistic models. A good analysis of the multiple wave dynamics may lead to a clearer understanding of the evolution of the epidemic, contributing to the development of strategies for reducing the propagation of the disease. To explore multi-wave impact, a classic epidemiological model, reflecting secondary infection wave emergence based on time-varying parameters, can be used. In this study, we present a new method to model multiple waves of infection within the COVID-19 epidemic. To capture the intricacies of epidemic dynamics, we propose using the generalized logistic model based on parameters varying over time.

Several factors motivated the choice of the generalized logistic model using time-dependent parameters for studying data relating to the COVID-19 outbreak. The nature of the COVID-19 pandemic, characterized by evolving trends and varying levels of transmission over time, necessitated a flexible modeling approach that could capture these dynamic changes. Traditional logistic models with fixed parameters might not adequately account for the temporal variations observed in the spread of the virus.

The use of time-varying parameters allows for a more nuanced analysis of the epidemic curve, enabling the model to adapt to fluctuations in infection rates, interventions, and other external factors influencing the trajectory of the outbreak. By incorporating time-dependent parameters, the model can better reflect the complex dynamics of the epidemic and provide more accurate predictions of future trends. Additionally, the generalized logistic model offers greater flexibility in capturing the different phases of the epidemic, including the initial exponential growth, the peak of transmission, and the eventual decline in cases. This versatility makes it well-suited for modeling the various stages of the COVID-19 pandemic and for providing insights into the effectiveness of public health measures and interventions.

Overall, the choice of the generalized logistic model based on time-dependent parameters was driven by the need for a robust and adaptable modeling framework capable of capturing the evolving dynamics of the COVID-19 outbreak and providing valuable insights for public health decision-making.

In Section 2, we present several epidemiological models, such as the Richards growth model, and the logistic model in addition to the generalized Richards model, illustrating each model parameter's impact and characteristics. These three models consider only constant parameters, without taking into account other factors such as human behavior, possible changes in the measures taken by governments to deal with the pandemic, and the appearance of several waves. In order to accurately reflect the dynamic aspects of the system, additional parameters representing both the effect of changes in government prevention measures as well as changes in the population's attitudes need to be included in the model. Section 3 is devoted to modeling the propagation of epidemics subject to multiple waves. All the models proposed in this section are generalizations of single-wave models using fixed parameters, in addition to the introduction of time-varying parameters. These models therefore incorporate the impact of public policies imposed by governments, such as social distancing, and changes in human behavior to control the pandemic.

Section 4 discusses the numerical methods for data analysis. A variety of mathematical models are used to carry out COVID-19 simulations, while forecasts of the propagation of the epidemic across different countries are provided on the basis of a reliable technique.

2. Single wave logistic models

In this section, we analyze the progression of the SARS-CoV-19 epidemic across various countries. We propose a series of logistic models to analyze the propagation of COVID-19 and thereby provide information on the situation of the pandemic. It is assumed that the equations and their associated parameters accurately predict and describe the cumulative progression of the infected population, even in the absence of additional variables. This assumption implies that the selected model adequately represents the underlying dynamics of the outbreak, thereby enabling the

generation of reliable predictions based solely on the provided parameters.

2.1. Logistic model

To describe the evolution of an epidemic at its outset, an exponential model can be used. Such a model has been used to characterize the initial phases of numerous epidemics, including Ebola, influenza, and the COVID-19 pandemic. Initially, the logistic model was introduced as part of Verhulst's [7] research into the growth pattern of the population. Epidemiology has made great use of this model to predict the emergence and spread of various diseases. The logistic model is defined as

$$\frac{d\,I(t)}{d\,t} = rI(t)\Big[1 - \frac{I(t)}{K}\Big], \tag{2.1}$$

In Eq 2.1, $I(t)$ represents the cumulative number of infected cases confirmed every day t, while K denotes the capacity or size limit of confirmed cases. It is well known that the solution to Eq (2.1) is given by

$$I(t) = \frac{KI(t_0)}{I(t_0) + (K - I(t_0))\exp(-r(t - t_0))} \tag{2.2}$$

where t_0 is the time when the first case $I(t_0)$ occurred, r is the exponential growth rate, and $I(t) \to K$ as $t \to \infty$. We observe that for $I(t) << K$, Eq (2.2) behaves as an exponential growth. However, when the total infected population $I(t)$ approaches K, the rate of growth is slow and tends to zero, giving rise to a symmetrical S-form curve. In other words, solution (2.2) to (2.1) is

$$I(t) = \frac{K}{1 + \exp(-r(t - t_0 - \tau))} \tag{2.3}$$

where $\tau = \dfrac{1}{r}\log\Big(\dfrac{K}{I(t_0)} - 1\Big)$ represents that the inflection point reached half of saturation, and $\Delta t = \dfrac{\log(81)}{r}$ is the measure of the time duration of the cycle from 10% to 90% of saturation. The advantage of this formula is that the parameters used are easy to interpret, and their value can be estimated before the closing of the evolution process. Thanks to expression (2.3), the daily number of infected cases is then calculated as follows:

$$I_f(t) := \frac{d\,I(t)}{d\,t} = \frac{rK\exp(-r(t - t_0 - \tau))}{\Big[1 + \exp(-r(t - t_0 - \tau))\Big]^2}. \tag{2.4}$$

Figure 1 shows the growth of infected individuals $I(t)$ over time for various values of the growth rate r with a fixed value of the carrying capacity K. It is clear that as r decreases, the peak moves to larger time values, and the maximum number of infected individuals is controlled. This leads to more efficient management of the pandemic.

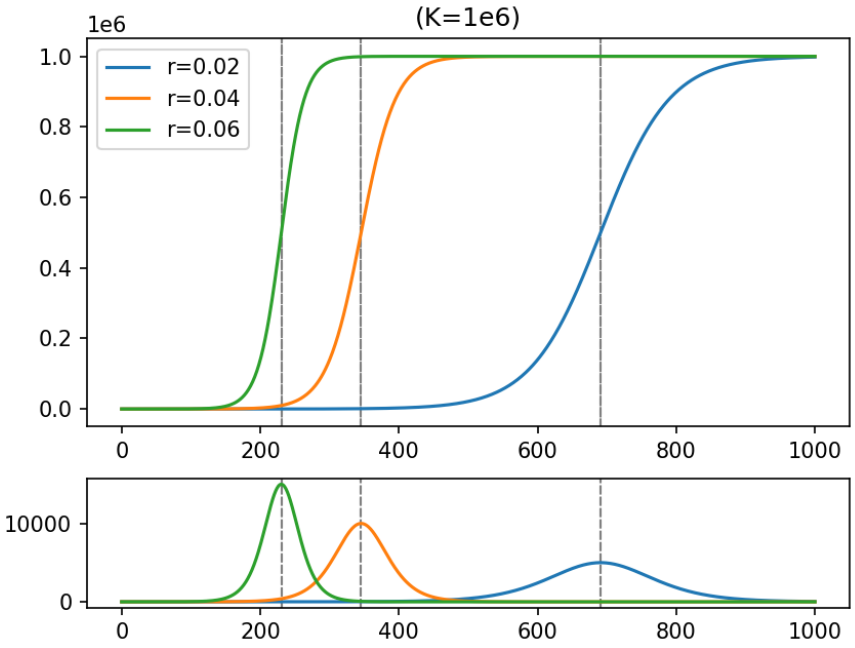

Figure 1. The cumulative infected (top) and number of infected (bottom) individuals per day with $K = 1e6$ and various values of the parameter r.

2.2. *Generalized logistic(Richards model)*

The preceding model depicts an S-shaped growth curve. Generalized logistic equations, however, are capable of modeling asymmetrical growth. They provide a flexible means of defining inflection points and describing various asymmetric degrees in the growth process. Richards's non-linear model is a highly versatile tool for characterizing various processes of growth [8–10], represents an extension of the logistic model, and is typically articulated through a nonlinear differential equation [11]. The equation representing the Richards growth model is expressed as

$$\frac{d\,I(t)}{d\,t} = rI(t)\Big[1 - \Big(\frac{I(t)}{K}\Big)^{\gamma}\Big] \tag{2.5}$$

where γ is a curve slope adjustment parameter. It is possible to calculate the solution by

$$I(t) = \frac{K}{\Big[1 + \exp(-\gamma r(t - t_0 - \tau))\Big]^{1/\gamma}} \tag{2.6}$$

where $\tau = \dfrac{1}{r\gamma}\log\Big((\dfrac{K}{I(t_0)})^{\gamma} - 1\Big)$.

This equation also has an exponential form, however the parameter $\gamma > 0$ in the equation allows the form of the upper part of the curve to be disconnected from the form of the lower part. The number of infected cases per day can be computed as

$$I_f(t) := \frac{d\,I(t)}{d\,t} = \frac{rK\exp(-r\gamma(t-t_0-\tau))}{\left[1+\exp(-r\gamma(t-t_0-\tau))\right]^{1+\frac{1}{\gamma}}}. \tag{2.7}$$

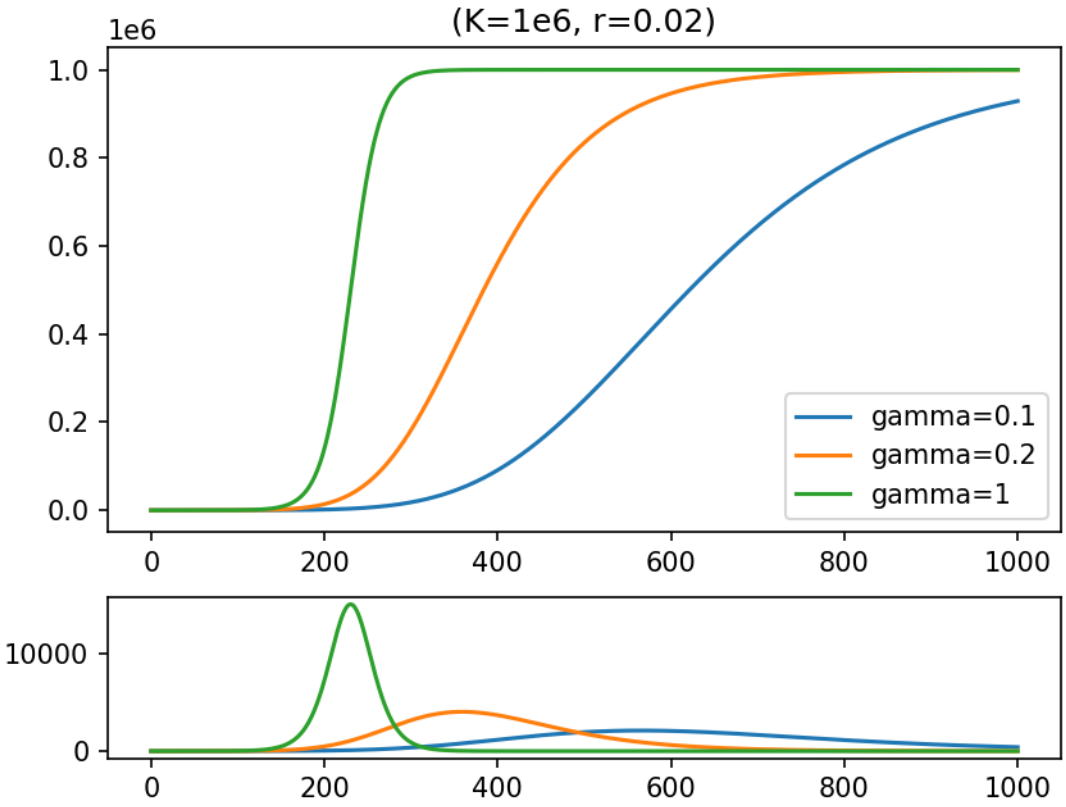

Figure 2. The cumulative infected (top) and the number of infected (bottom) individuals per day with $K = 1e6$, $r = 0.02$, and various values of γ.

Figure 2 illustrates the growth of the cumulative and daily infected cases for various values of the parameter γ with a fixed value of the growth rate r and fixed carrying capacity.

Expanding on the Richards growth model (2.5), the generalised Richards model (GRM) introduces a supplementary parameter p as

$$\frac{d\,I(t)}{d\,t} = rI^p(t)\Big(1-\Big(\frac{I(t)}{K}\Big)^{\gamma}\Big). \tag{2.8}$$

In Figure 3, we fix the values of the parameters γ, growth rate r, and carrying capacity K. We present the growth of infected cases for different values of the parameter p.

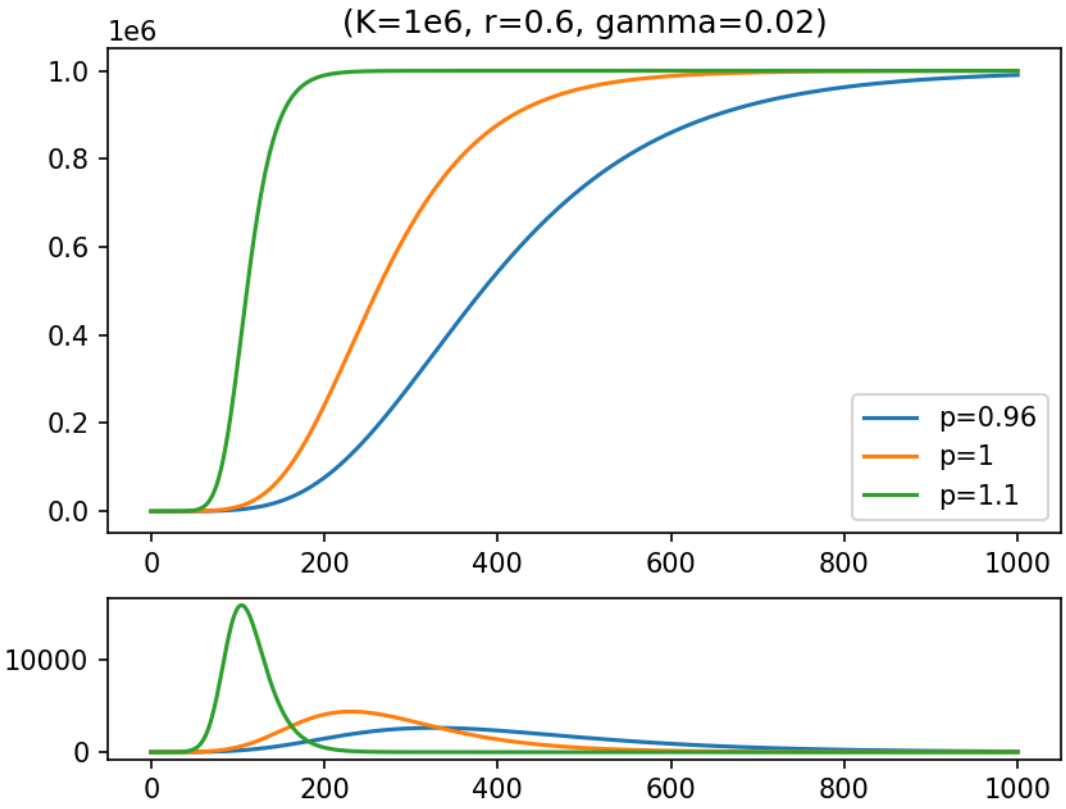

Figure 3. The cumulative infected (top) and number of infected (bottom) per day individuals with $K = 1e6$, $r = 0.6$, $\gamma = 0.02$, and various values of p.

3. Multi-wave models with time-dependent parameters

The models described above are applied only to a single growth period, during which the system undergoes a transition from rapid to slower growth upon reaching a carrying capacity K. Nevertheless, such models do not consider the influence of the government policy changes adopted to deal with the pandemic and human attitudes, both of which can lead to several periods of growth in various countries. The model must therefore take into account both human behaviour and measures taken by public authorities. To achieve this, the governing equations and systems should treat variables such as carrying capacity and growth rates as a function of time. Therefore, any change in the public authorities' measures or strategies will be automatically reflected in the predicted number of infected cases by the model.

The resulting model is a set of nonlinear coupled equations and systems. This section describes Meyer's bi-logistics model to simulate growth when load capacity varies [12]. The model consists of two serial logistic growth periods, each of which can be modeled with a logistic function. The time interval can be split into two subregions, and each subregion can be modeled with a logistic function.

$$I(t) = \frac{K_1}{1 + \exp(-r_1(t - t_0 - \tau_1))} + \frac{K_2}{1 + \exp(-r_2(t - t_0 - \tau_2))} \tag{3.1}$$

where $\tau_i = \frac{1}{r_i} \log\Big((\frac{K_i}{I(t_0)}) - 1\Big)$ for $i = 1, 2$.

A more general approach was proposed in [13] using a combination of the Richards equations:

$$I(t) = \sum_{i=1}^{m} \frac{K_i}{\Big[1 + \exp(-\gamma_i r_i(t - t_0 - \tau_i))\Big]^{1/\gamma_i}}, \tag{3.2}$$

where $\tau_i = \frac{1}{r_i\gamma_i} \log\Big((\frac{K_i}{I(t_0)})^{\gamma_i} - 1\Big)$ for $i = 1, ..., m$.

One drawback of this approach is the difficulty in finding the appropriate time to separate the regions and the lack of clarity in the separation between each process.

To address this issue, [13] proposed a new mathematical model (**Model 1**) that takes into account changes in the strategy of the public authorities by assuming that the variable p is dependent on time t such that

$$\frac{d\,I(t)}{d\,t} = rI^{p(t)}(t)\Big[1 - \Big(\frac{I(t)}{K}\Big)^{\gamma}\Big]. \tag{3.3}$$

In the event that social distancing measures are in place, it is possible to describe human behavioral dynamics by varying $p(t)$ and $K(t)$ across time. [13] introduced a more adaptive model (**Model 2**) given by

$$\frac{d\,I(t)}{d\,t} = rI_c^{p(t)}(t)\Big[1 - \Big(\frac{I(t)}{K(t)}\Big)^{\gamma}\Big]. \tag{3.4}$$

To improve the results obtained in [13], we propose a new mathematical model that assumes that variables $p(t)$ and $r(t)$ are dependents on time t such that

$$p(t) = \begin{cases} p_1 & \text{if} \quad t \le t_1 \\ p & \text{if} \quad t_1 \le t \le t_2 \\ p_2 & \text{if} \quad t \ge t_2 \end{cases} \tag{3.5}$$

and

$$r(t) = \begin{cases} r_1 & \text{if} \quad t \le t_3 \\ r & \text{if} \quad t_3 \le t \le t_4 \\ r_2 & \text{if} \quad t \ge t_4. \end{cases} \tag{3.6}$$

$p(t)$ and $r(t)$ are a piece-wise and discontinuous functions. We will now consider the regularized nonlinear problem, which can be expressed as:

$$\frac{d\,I(t)}{d\,t} = r_\varepsilon(t)I^{p_\varepsilon(t)}(t)\Big[1 - \Big(\frac{I(t)}{K}\Big)^{\gamma}\Big] \tag{3.7}$$

where $p_\varepsilon(t) := p(t) * \zeta_\varepsilon(t) = \int_{-\infty}^{\infty} p(\tau)\zeta_\varepsilon(t - \tau)d\tau$ and $r_\varepsilon(t) := r(t) * \zeta_\varepsilon(t) = \int_{-\infty}^{\infty} r(\tau)\zeta_\varepsilon(t - \tau)d\tau$ are regularizations of $p(t)$ and $r(t)$, respectively, and $\zeta_\varepsilon(t) := \frac{1}{\varepsilon}\zeta(\frac{t}{\varepsilon})$. ζ is defined by

$$\zeta(t) = \begin{cases} \frac{1}{a}\exp(\frac{1}{t^2-1}) & \text{if} \quad -1 \le t \le 1 \\ 0 & \text{elsewhere} \end{cases} \tag{3.8}$$

with $a = \int_{-1}^{1} \exp(-\frac{1}{1-t^2})dt$.

By also varying $K(t)$ over time, a more adaptive model (**Model 3**) can be introduced:

$$\frac{d\,I(t)}{d\,t} = r_\varepsilon(t)I_c^{p_\varepsilon(t)}(t)\Big(1 - (\frac{I(t)}{K(t)})^\gamma\Big) \tag{3.9}$$

where $K(t)$ satisfies

$$\frac{d\,K(t)}{d\,t} = v(K(t) - K_1)\Big(1 - \Big[\frac{K(t) - K_1}{K_2}\Big]^\mu\Big). \tag{3.10}$$

Let $\frac{dI(t)}{dt} = I_f(t)$, then the derivative of $I_f(t)$ is given by

$$\begin{aligned} \frac{dI_f(t)}{dt} &= I^{p_\varepsilon(t)}\Big[\Big(\frac{d\,r_\varepsilon(t)}{d\,t} + r_\varepsilon(t)\frac{dp_\varepsilon(t)}{dt}\log(I(t))\Big)\Big(1 - \Big(\frac{I(t)}{K(t)}\Big)^\gamma\Big) + \gamma r_\varepsilon(t)\frac{d\log(K(t))}{dt}\Big(\frac{I(t)}{K(t)}\Big)^\gamma \\ &\quad + (r^2)_\varepsilon(t)I^{p_\varepsilon(t)-1}\Big(p_\varepsilon(t) - (p_\varepsilon(t)+\gamma)\Big(\frac{I(t)}{K(t)}\Big)^\gamma\Big)\Big(1 - \Big(\frac{I(t)}{K(t)}\Big)^\gamma\Big)\Big]. \end{aligned} \tag{3.11}$$

Then (3.11) becomes

$$\begin{cases} \frac{dI_f(t)}{dt} &= I_c^{p_\varepsilon(t)}\Big[\Big(\frac{d\,r_\varepsilon(t)}{d\,t} + r_\varepsilon(t)\frac{dp_\varepsilon(t)}{dt}\log(I(t))\Big)\Big(1 - \Big(\frac{I(t)}{K(t)}\Big)^\gamma\Big) + \gamma r_\varepsilon(t)\frac{d\,log(K(t))}{dt}\Big(\frac{I(t)}{K(t)}\Big)^\gamma \\ &\quad + (r_\varepsilon)^2(t)I^{p_\varepsilon(t)-1}\Big(p_\varepsilon(t) - (p_\varepsilon(t)+\gamma)\Big(\frac{I(t)}{K(t)}\Big)^\gamma\Big)\Big(1 - \Big(\frac{I(t)}{K(t)}\Big)^\gamma\Big)\Big] \\ \frac{dI(t)}{dt} &= r_\varepsilon(t)I^{p_\varepsilon(t)}(t)\Big[1 - \Big(\frac{I(t)}{K(t)}\Big)^\gamma\Big] \\ \frac{d\,K(t)}{d\,t} &= v(K(t) - K_1)\Big(1 - \Big[\frac{K(t) - K_1}{K_2}\Big]^\mu\Big). \end{cases} \tag{3.12}$$

The solution to Eq (3.12) is

$$K(t) = K_1 + \frac{K_2}{\Big[1 + \exp(-\mu v(t - t_0 - \tau))\Big]^{1/\mu}} \tag{3.13}$$

where $\tau = \frac{1}{\mu v}\log\Big(\Big[\frac{K_2}{K_0 - K_1}\Big]^\mu - 1\Big)$ and

$$K_1 \le K_0 := K(t_0) \le K_1 + K_2.$$

The equation of $I(t)$ can be expressed as

$$\begin{cases} \dfrac{dI(t)}{dt} & = r_\varepsilon(t) I^{p_\varepsilon(t)}(t)\Big[1 - \Big(\dfrac{I(t)}{K(t)}\Big)^\gamma\Big] := \mathcal{F}_\varepsilon(t,\ I(t)) \\ \\ I(0) & = I_0. \end{cases} \tag{3.14}$$

The solutions $I(t) = 0$ and $I(t) = K(t)$ are the equilibrium solutions of the previous equation. For Eq (3.14), starting with a positive initial population $0 < I_0 \leq K(t)$. Now let $\tilde{\mathcal{F}}_\varepsilon$, be defined as

$$\tilde{\mathcal{F}}_\varepsilon(t,\ I(t)) = \begin{cases} \mathcal{F}_\varepsilon(t,\ I(t)) & \text{if } I(t) \geq 0 \\ \\ 0 & \text{else} \end{cases} \tag{3.15}$$

and $\tilde{I}(t)$, be a solution to

$$\begin{cases} \dfrac{d\tilde{I}(t)}{dt} & = \tilde{\mathcal{F}}_\varepsilon(t,\ \tilde{I}(t)) \\ \\ \tilde{I}(0) & = I_0. \end{cases} \tag{3.16}$$

Multiplying equation (3.16) by $(\tilde{I}(t) - K(t))^+ = max\{\tilde{I}(t) - K(t), 0\}$, we obtain

$$\frac{dI(t)}{dt}(\tilde{I}(t) - K(t))^+ = \tilde{\mathcal{F}}_\varepsilon(t,\ \tilde{I}(t))\ (\tilde{I}(t) - K(t))^+.$$

Then we have

$$\frac{1}{2}\frac{d}{dt}|(\tilde{I}(t) - K(t))^+|^2 + \frac{dK(t)}{dt}(\tilde{I}(t) - K(t))^+ = \tilde{\mathcal{F}}_\varepsilon(t,\ \tilde{I}(t))\ (\tilde{I}(t) - K(t))^+ \leq 0.$$

We have $K_1 \leq K(t) \leq K_1 + K_2$ and, from the last equation in (3.12), we have $\frac{dK(t)}{dt} \geq 0$. Then

$$\frac{1}{2}\frac{d}{dt}|(\tilde{I}(t) - K(t))^+|^2 \leq 0.$$

Since the initial data $I_{c,0} \leq K(t)$, we deduce that $(\tilde{I}(t) - K(t))^+ = 0$, and $\tilde{I}(t) \leq K(t)$. On the other hand, we have $1 - \Big(\dfrac{I(t)}{K(t)}\Big)^\gamma \geq 0$ and, from (3.16), we obtain $\tilde{\mathcal{F}}_\varepsilon(t,\ I(t))$, and $\dfrac{d\tilde{I}(t)}{dt} \geq 0$. Since the initial data $I_{c,0}$ is nonnegative, we deduce that $\tilde{I}(t) \geq I_{c,0} > 0$. Consequently, $0 < \tilde{I}(t) \leq K(t)$ and also $0 < I(t) \leq K(t)$.

4. Numerical simulations

The objective of this section is to meticulously identify the fundamental parameters that are necessary for the proposed epidemic models. These parameters are of paramount importance in forecasting as they constitute the foundation of the model's predictive capabilities. Given the dynamic nature of public authorities' policies and actions concerning the pandemic, it is probable that these parameters will fluctuate over time.

In this investigation, we utilized data sourced from a Git repository affiliated with Johns Hopkins University, as cited in references [14–16]. The x-axis across all subsequent visualizations represents the number of days elapsed since January 22, 2020.

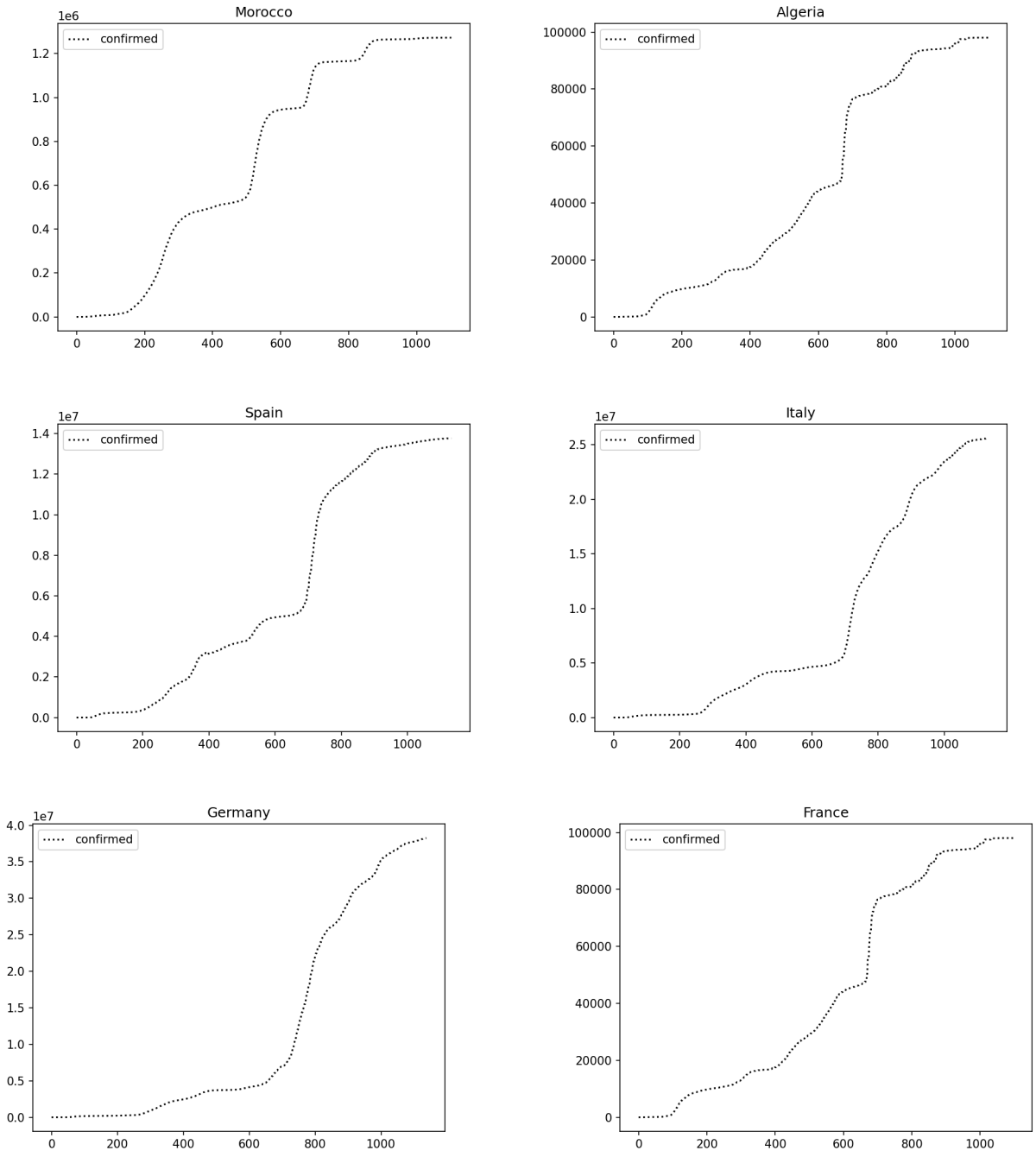

Figure 4. Cumulative cases in Morocco, Algeria, Spain, Italy, Germany, and France.

The graphs depicted in Figure 4 illustrate the cumulative rise in cases during the initial stages of the epidemic across various countries, including Morocco, Algeria, Spain, Italy, Germany, and France. It

is evident that the pandemic is exhibiting exponential growth patterns, underscoring the necessity for decisive interventions by public authorities to mitigate its impact.

4.1. Parameters estimation

The process of obtaining model parameters involves executing a least-squares fit on the observed data, as outlined in [17]. This process involves identifying the parameter set that minimizes the sum of squared variances between the actual data and the corresponding model solution. In essence, the objective is to fine-tune the model's parameters to achieve optimal alignment with the empirical data, thereby optimizing the model's predictive capability.

In order to assess the efficacy of the models applied to the data, we calculate the temporal fluctuation of the residuals, which is represented as follows:

$$\mathcal{R}esidual(t_j) = I_c^{\vartheta_\varepsilon}(t_j) - I_d(t_j) \tag{4.1}$$

where $\vartheta^\star$ is the value of the estimated parameters. To evaluate the error associated with forecasts, one can compute the error of various models fit to the data, by using the mean absolute error (MAE)

$$MAE := \frac{1}{m}\sum_{j=1}^{m} |I_c^{\vartheta^\star}(t_j) - I_d(t_j)| \tag{4.2}$$

or the mean squared error (MSE)

$$MSE := \frac{1}{m}\sum_{j=1}^{m} |I_c^{\vartheta^\star}(t_j) - I_d(t_j)|^2. \tag{4.3}$$

4.2. Results

To demonstrate the efficacy of the proposed model, we conducted parameter fitting using datasets from a variety of countries, including Morocco, Algeria, Spain, Italy, Germany, and France. This comprehensive strategy permitted the evaluation of the model's performance across a spectrum of epidemiological contexts and diverse public health interventions. The inclusion of a diverse array of data sources ensures a robust assessment of the model's adaptability and predictive capability across a range of scenarios and geographic regions.

The research involved an extensive series of tests, utilizing over 1000 days worth of data. The objective of these tests was to demonstrate the efficacy of the proposed models in accurately forecasting scenarios involving multiple waves of the epidemic.

In our research, we heavily relied on two indispensable Python packages for conducting simulations:

- lmfit: This robust Python package offers a sophisticated interface tailored for curve fitting and parameter estimation. Especially adept at fitting models to experimental data, 'lmfit' facilitates the extraction of significant parameters from these fits. Its flexibility allows users to define custom models and constraints with ease, while its nonlinear least squares optimization framework simplifies the process. Notably, 'lmfit' employs robust fitting techniques, enhancing resilience to outliers. This is particularly advantageous, as it provides options like the robust parameter within the minimize function, which further fortifies its capabilities.

- SciPy's 'scipy.integrate.odeint': Widely acclaimed across scientific and engineering domains, the 'scipy.integrate.odeint' function, housed within the SciPy library, is an indispensable tool for numerically tackling ordinary differential equations (ODEs). Its versatility has led to its widespread adoption in simulating dynamical systems with remarkable success.

It is worth noting that while utilizing the 'lmfit' package, the robust fitting techniques embedded within it contribute to greater resilience against outliers. The availability of robust fitting options, such as the robust parameter within the minimization function, bolsters its effectiveness.

Furthermore, it is important to acknowledge that the accuracy of the results obtained may be marginally influenced by the initial guess of the parameters.

Figures 5 and 6 serve as visual demonstrations of the superior performance of the proposed models compared to the logistic model and Richard growth model. Unlike these traditional models, which are limited to capturing only a single pandemic wave, the proposed models exhibit adaptability to multiple-wave pandemics. Additionally, Figure 6 provides insight into the time-dependent parameters $p(t)$ and $r(t)$ resulting from the proposed models, further illustrating their versatility and effectiveness in modeling complex epidemic scenarios.

The process of evaluating regression models is fundamental to understanding their effectiveness in predicting or elucidating relationships among variables. This process entails the application of various techniques that are specifically designed to achieve this objective. In our investigation, we concentrated on two metrics that are frequently employed in this context: The mean squared error (MSE) and the mean absolute error (MAE) were employed.

The mean squared error (MSE) is a metric that provides a comprehensive assessment of predictive accuracy by measuring the average squared disparity between predicted and actual values. In contrast, MAE calculates the average absolute difference between predicted and actual values, offering a more intuitive perspective on model performance.

Throughout the course of our investigation, we employed these metrics to assess the predictive capabilities of a range of regression models. Lower values for both MSE and MAE indicate a closer alignment between predicted and actual values, thereby reflecting heightened accuracy in capturing the underlying relationships within the data. This meticulous evaluation process serves as a crucial step in ensuring the reliability and robustness of regression models for real-world applications.

Figures 7 and 8 depict a comparison among all discussed models. It is evident that models incorporating time-dependent parameters exhibit superior performance.

In Figures 7 and 8, a comprehensive comparison is presented among all discussed models. It is evident that models integrating time-dependent parameters (model 1, model 2, and model 3) exhibit superior performance. This observation highlights the necessity of accounting for temporal dynamics in modeling processes, as it leads to more accurate predictions and a more comprehensive understanding of complex phenomena. The visual representation provided by these figures serves to reinforce the significance of incorporating such parameters into regression models for the purpose of improving predictive capabilities.

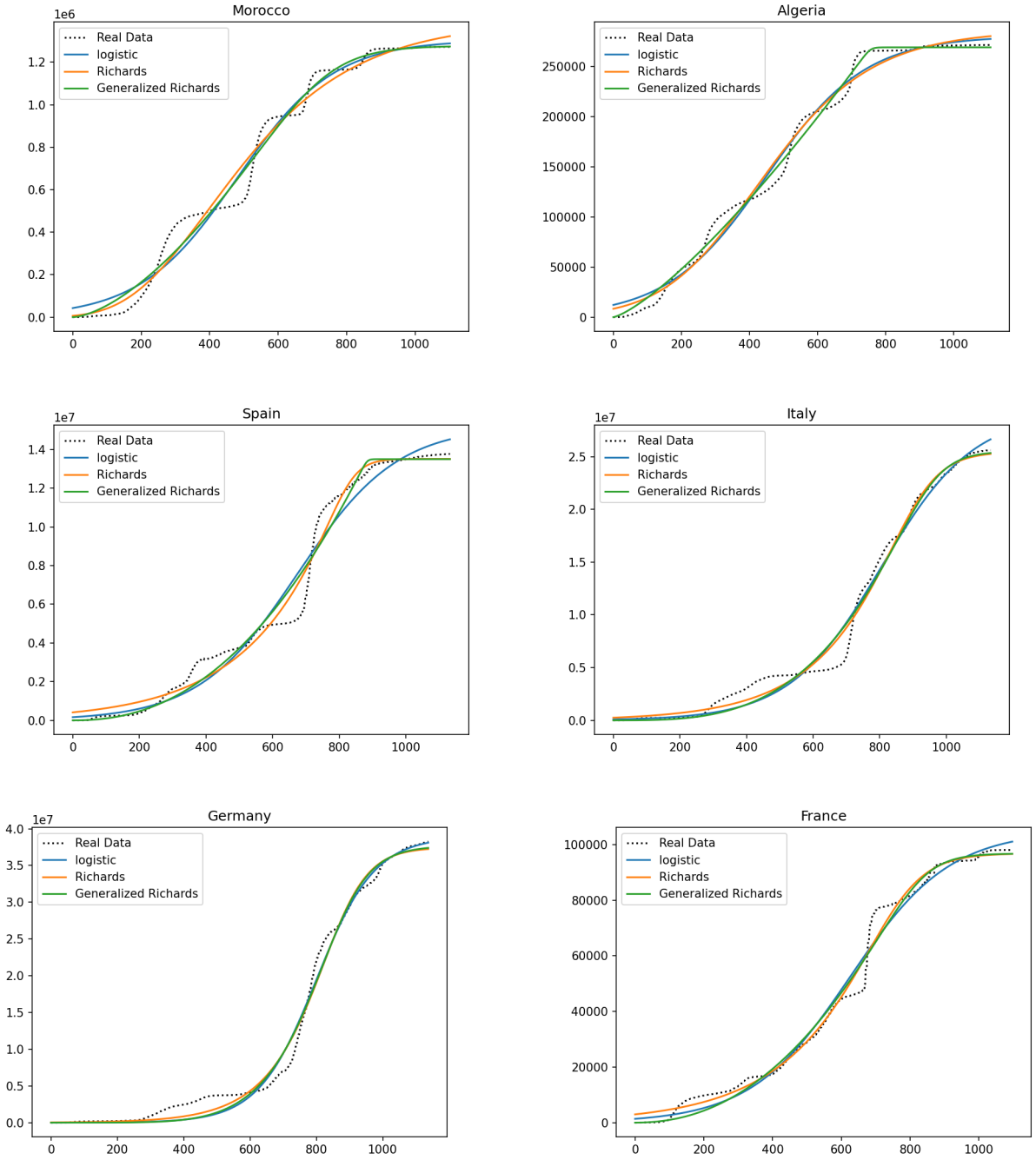

Figure 5. Application of logistic models to fit data from Morocco, Algeria, Spain, Italy, Germany, and France.

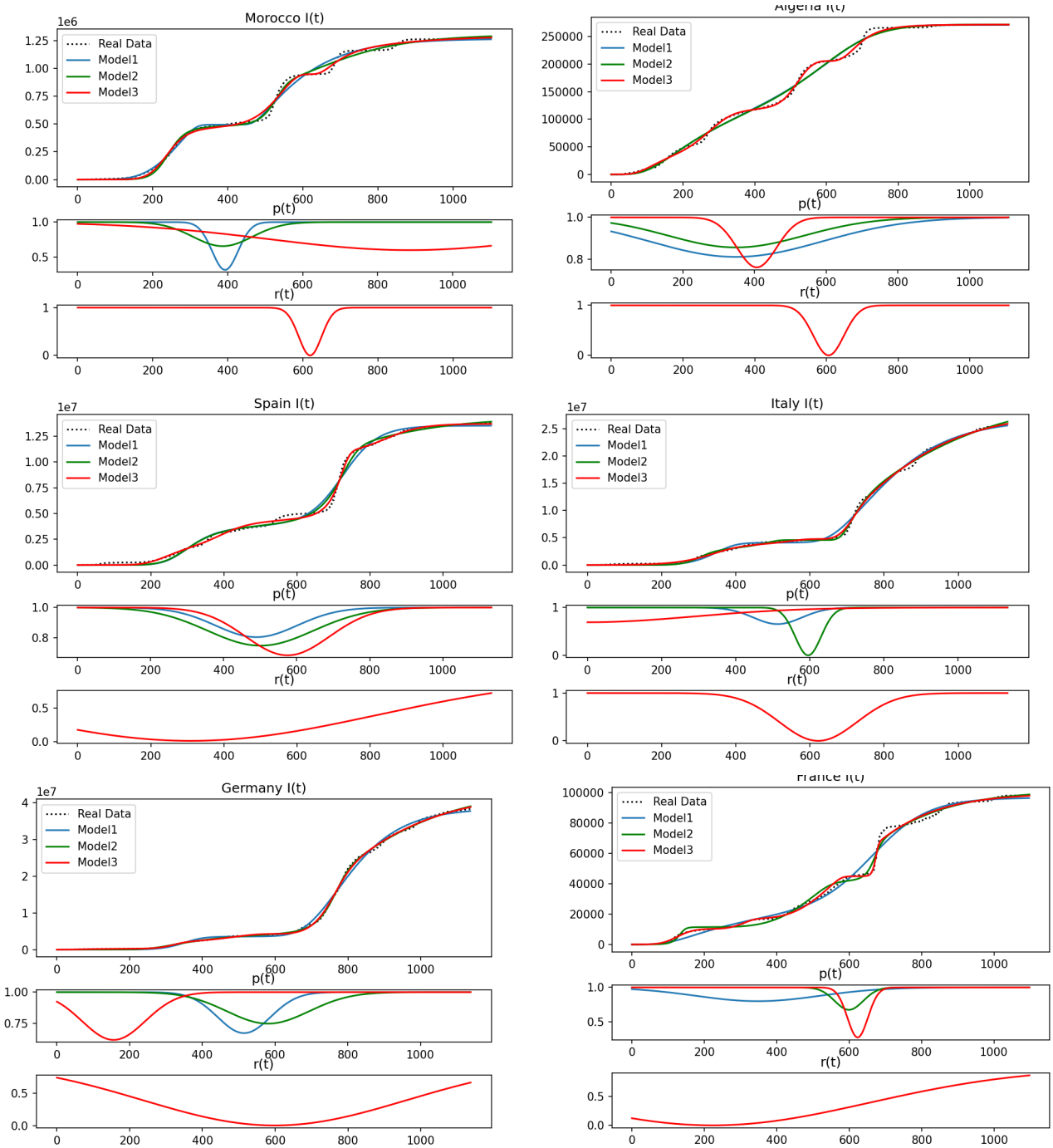

Figure 6. Application of logistic models with time-dependent parameters to fit data from Morocco, Algeria, Spain, Italy, Germany, and France.

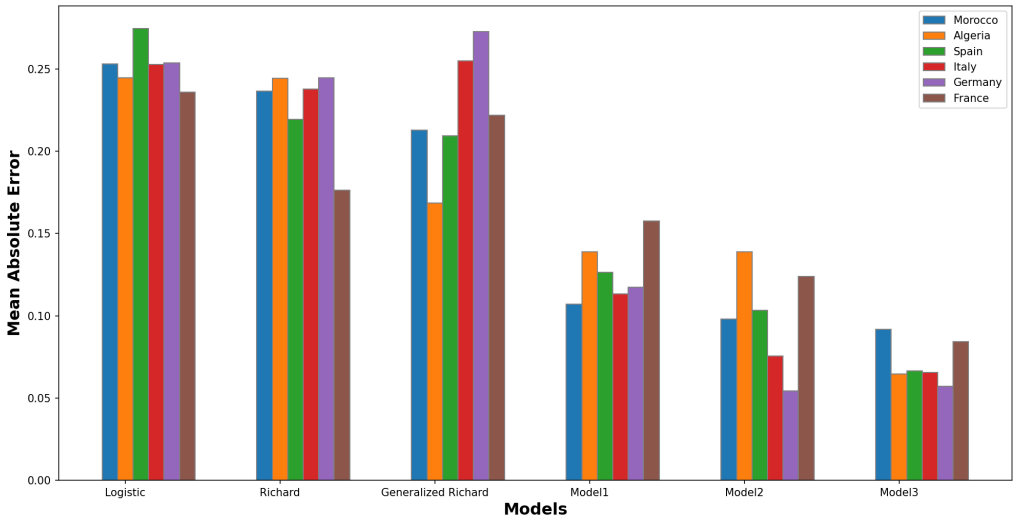

Figure 7. Comparison of the mean absolute error of different models for different countries.

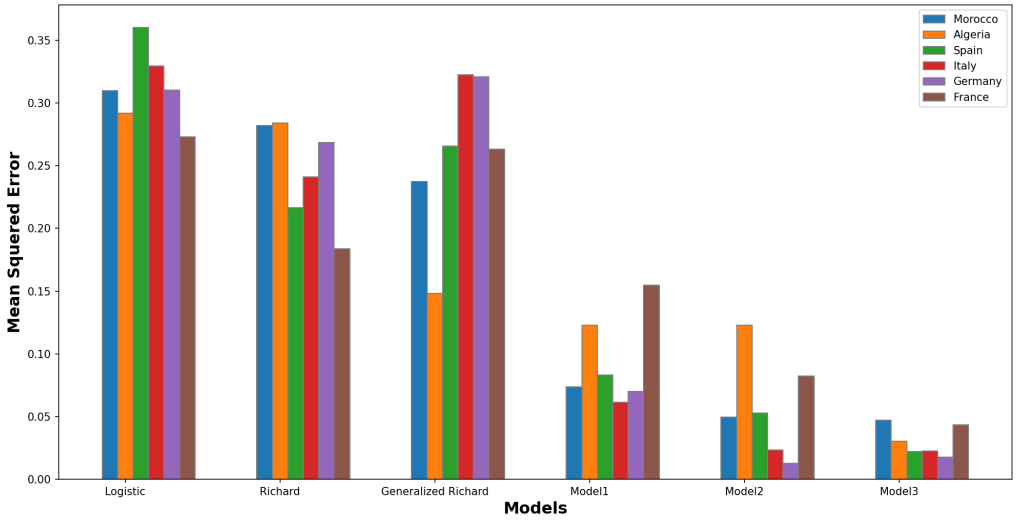

Figure 8. Comparison of the mean squared error of different models for different countries.

4.3. Implications and limitations of study

Observations reveal that various waves of the pandemic exhibit distinct behaviors; hence, a traditional model often struggles to accurately predict and track the impacts across different waves. Introducing supplementary variables that are time-dependent can significantly enhance the model's ability to manage and forecast the evolution of the pandemic more effectively. By dynamically

adjusting these variables over time, the model becomes more adaptable, capturing the nuances and shifts inherent in each wave of the pandemic. This approach not only improves the accuracy of predictions but also offers a more comprehensive understanding of how the pandemic evolves over time.

The incorporation of time-dependent parameters into our proposed model offers significant flexibility, enabling more precise modeling and a nuanced capacity to track the pandemic's progression. However, in this study, we opted for piece-wise constant functions, $p(t)$ and $r(t)$, to describe various phases of the pandemic. This decision permitted the determination of these values through fitting procedures. Nevertheless, it is crucial to recognize that the broader scenario remains highly complex, akin to an open problem that resembles an inverse problem. This implies that inferring the underlying parameters from observed data remains a challenging task with ongoing research implications.

5. Conclusions

The development of precise prediction techniques to anticipate and forecast the transmission of infectious diseases represents a significant challenge. It necessitates a comprehensive examination of contagion parameters, model uncertainty, and real-world data. This necessitates not only an understanding of the dynamics of disease transmission but also the ability to grapple with the inherent uncertainties in predictive modeling and the complexities of incorporating real-time data into those models. The successful development of these techniques will greatly enhance our ability to proactively manage and mitigate the impact of epidemics and pandemics.

This paper presents a robust suite of forecasting models aimed at predicting the trajectory of the novel coronavirus (COVID-19) as it spreads across various countries worldwide. Specifically, we examine the efficacy of dynamic differential equation models in capturing the complex dynamics of the pandemic. Our approach incorporates a diverse set of forecasting tools, including logistic models and multiple cycle models (designated as models 1, 2, and 3), which have been tailored to offer short-term forecasts for COVID-19 epidemics.

These models are designed to adapt to the evolving nature of the pandemic by integrating flexible epidemic growth scaling. By employing the power of differential equations and incorporating various parameters that influence disease spread, our methodology provides a comprehensive framework for anticipating the trajectory of COVID-19 outbreaks across different regions. Through rigorous testing and validation, we demonstrate the effectiveness of our approach in providing timely and accurate forecasts to aid public health decision-making and resource allocation efforts.

Using these models provides valuable information on the evolution of COVID-19, offering essential guidance for the formulation of public health policies in order to reduce transmission of the virus. Although the analysis is primarily focused on the second wave, the model's flexibility allows for its expansion to accommodate any number of subsequent waves. This adaptability renders it an invaluable asset for understanding and addressing the complex challenges posed by the COVID-19 pandemic. The model offers insights into the dynamics of successive waves, providing researchers and policymakers with valuable information to devise more effective strategies for containment and mitigation efforts.

This work uses time-dependent parameters, so we used a piece-wise function. We believe that the use of more complex functions can improve model performance. We could also extend the work by

introducing vaccination and spatial interaction using non-local diffusion operators.

Author contributions

Said Gounane, Jamal Bakkas, Mohamed Hanine, Gyu Sang Choi and Imran Ashraf: Writing – original draft, Writing – review & editing. The authors contributed equally to the writing of this paper. All authors have read and agreed to the published version of the manuscript.

Use of AI tools declaration

The authors declare that they have not used Artificial Intelligence tools in the creation of this article.

Acknowledgments

This work was supported by Basic Science Research Program through the National Research Foundation of Korea (NRF) funded by the Ministry of Education (NRF-2021R1A6A1A03039493).

Conflict of interest

The authors declare there is no conflict of interest.

References

1. G. Chowell, Fitting dynamic models to epidemic outbreaks with quantified uncertainty: A primer for parameter uncertainty, identifiability, and forecasts, *Infect. Dis. Modell.*, **2** (2017), 379–398.
2. H. Heesterbeek, R. M. Anderson, V. Andreasen, S. Bansal, D. De Angelis, C. Dye, et al., Modeling infectious disease dynamics in the complex landscape of global health, *Science*, **347** (2015), aaa4339. https://doi.org/10.1126/science.aaa4339
3. S. Funk, M. Salathe, V. A. A. Jansen, Modelling the influence of human behaviour on the spread of infectious diseases: A review, *J. Royal Soc., Interface* , **7** (2010), 1247–1256.
4. C. Poletto, M. Gomes, Y. P. A. Pastore, L. Rossi, L. Bioglio, D. Chao, et al., Assessing the impact of travel restrictions on international spread of the 2014 West African Ebola epidemic, *Eurosurveillance*, **19** (2014).
5. D. Okuonghae, A. Omame, Analysis of a mathematical model for COVID-19 population dynamics in Lagos, Nigeria, *Chaos, Solution. Fract.*, **139** (2020), 110032.
6. A. Omame, D. Okuonghae, U. K. Nwajeri, C. P. Onyenegecha, A fractional-order multi-vaccination model for COVID-19 with non-singular kernel, *Alexandria Eng. J.*, **61** (2022), 6089–6104. https://doi.org/10.1016/j.aej.2021.11.037
7. S. F. Verhulst, *Notice sur la loi que la population suit dans son accroissement. Corr. Math.Physics.* 10 (1838) 113.

8. H. Ghosh, M. A. Iquebal, Prajneshu, Bootstrap study of parameter estimates for nonlinear Richards growth model through genetic algorithm, *J. Appl. Stat.*, **38** (2011), 491–500. https://doi.org/10.1080/02664760903521401
9. J. Lv, K. Wang, J. Jiao, Stability of stochastic Richards growth model, *Appl. Math. Modell.*, **39** (2015), 4821–4827. https://doi.org/10.1016/j.apm.2015.04.016
10. X. Wang, J. Wu, Y. Yang, Richards model revisited: Validation by and application to infection dynamics, *J. Theor. Biol.*, **313** (2012), 12–19. https://doi.org/10.1016/j.jtbi.2012.07.024
11. G. Himadri, Prajneshu, Optimum Fitting of Richards Growth Model in Random Environment, *J. Stat. Theory Pract.*, **13** (2019), 6.
12. P. Meyer, Bi-logistic growth, *Technol. Forecast. Soc. Change*, **47** (1994), 89–102. https://doi.org/10.1016/0040-1625(94)90042-6
13. S. Gounane, J. Bakkas, F. Karami, Y. Barkouch, Nonlinear Growth Models with Lockdown Periods for Analyzing Cumulative and Daily COVID-19 Outbreak Data, *IEEE International Conference on Advances in Data-Driven Analytics And Intelligent Systems (ADACIS)* , 2023, 1–6. http://doi.org/10.1109/ADACIS59737.2023.10424370
14. GitHub, Covid-19 repository at github, 2020. Available from: `https://github.com/CSSEGISandData/COVID-19`.
15. E. Dong, H. Du, L. Gardner, An interactive web-based dashboard to track COVID-19 in real time, *Lancet Infect. Dis.*, **20** (2020), 533–534. https://doi.org/10.1016/S1473-3099(20)30120-1
16. E. Dong, J. Ratcliff, T. D. Goyea, A. Katz, R. Lau, T. K. Ng, et al., The Johns Hopkins University Center for Systems Science and Engineering COVID-19 Dashboard: Data collection process, challenges faced, and lessons learned, *Lancet. Infect. Dis.*, **22** (2022), e370–e376. https://doi.org/10.1016/S1473-3099(22)00434-0
17. H. T. Banks, S. Hu, W. C. Thompson, *Modeling and inverse problems in the presence of uncertainty*, New York: Chapman and Hall/CRC, 2014.

AIMS Press